HHS Public Access

Author manuscript

Curr Opin Chem Biol. Author manuscript; available in PMC 2019 July 03.

Published in final edited form as:

Curr Opin Chem Biol. 2018 August ; 45: 113–120. doi:10.1016/j.cbpa.2018.03.017.

Molecular imaging agents for ultrasound

Aimen Zlitni[1] and **Sanjiv S Gambhir**[1,2]

[1]Department of Radiology, Molecular Imaging Program at Stanford, Canary Center at Stanford for Cancer Early Detection, Stanford University, Stanford, CA, United States

[2]Department of Bioengineering, Department of Materials Science and Engineering, Stanford University, Stanford, CA, United States

Abstract

Ultrasound (US) imaging is a safe, sensitive and affordable imaging modality with a wide usage in the clinic. US signal can be further enhanced by using echogenic contrast agents (UCAs) which amplify the US signal. Developments in UCAs which are targeted to sites of disease allow the use of US imaging to provide molecular information. Unfortunately, traditional UCAs are too large to leave the vascular space limiting the application of molecular US to intravascular markers. In this mini review, we highlight the most recent reports on the application of molecular US imaging in the clinic and summarize the latest nanoparticle platforms used to develop nUCAs. We believe that the highlighted technologies will have a great impact on the evolution of the US imaging field.

Introduction

Ultrasound imaging (US) is the second most widely used medical imaging modality due to its high sensitivity, portability, relative low cost, and good safety profile (no ionizing radiation) [1]. In US imaging, anatomical images are produced after measuring the propagation of high frequency sound waves when travelling between materials and tissue interfaces of different acoustic properties [1]. Contrast enhanced ultrasound (CEUS) takes advantage of using highly echogenic contrast agents to further amplify the US signal allowing imaging organs with low US contrast (i.e. blood pool) [2]. Ultrasound contrast agents (UCAs) are typically gas-filled micronsized bubbles (MBs) with a 1–8 *m*m diameter which oscillate upon interacting with the US wave thus enhancing the reflected US signal. To date, seven MBs have been approved for clinical use and are routinely utilized to improve organ imaging and to better assess blood flow and vascularization [2–4]. In the past two decades, many efforts focused on developing MBs which are targeted to vascular endothelial markers of disease by attaching biomolecules to its surface expanding the utility of CEUS in the molecular imaging field [5●]. Preclinical validation of molecular US imaging of a variety of diseases such as inflammation (inflammatory bowel disease, myocardial ischemia, atherosclerosis and cardiac transplant rejection) and cancer (pancreatic, angiosarcoma, ovarian, prostate, breast, colon, liver, renal, glioma and melanoma) have been reported [5●]. In addition, advances in transducer technology and pulse sequences stimulated the use of CEUS for therapy through ultrasound-mediated bubble destruction. Such innovations are now widely employed to reversibly break the blood–brain barrier, cause cavitation and enhance site specific drug/gene delivery with improved therapeutic outcomes [6].

Unfortunately, current UCAs cannot extravasate beyond the vasculature due to their micron-size and have limited circulation time constraining the advancement of molecular US imaging (Figure 1a). In this review, the first application of targeted MBs for molecular US imaging of disease in the clinic will be summarized and recent efforts in the development of the next generation of nano-sized UCAs (nUCAs) will be highlighted.

Molecular US imaging in the clinic

To date there is only one molecularly targeted UCA that is being evaluated in the clinic. This contrast agent, named BR55 (Bracco, Italy), has a mean diameter of 1.5 μm and is composed of a phospholipid shell and a gas core consisting of perfluorobutane and nitrogen. BR55 is targeted to kinase insert domain receptor (KDR) which is a human analog of vascular endothelial growth factor receptor type 2 (VEGFR2) a known marker overexpressed in many human cancer types [7]. After an extensive preclinical evaluation of BR55 by various groups and in multiple animal models, BR55 is now being evaluated in humans for prostate, ovarian, pancreatic, and breast cancer imaging. Our group published their first in human results showing the efficacy and safety of BR55 in evaluating patients with breast ($n = 21$) and ovarian ($n = 24$) cancer lesions [8••]. After BR55 injection and ultrasound imaging for up to 29 min, tissue samples were taken out in order to correlate the KDR-expression observed indirectly via the US image with that observed through direct immunohistochemistry (IHC) staining. The US image signal matched well with KDR-expression on IHC (93% of breast and 85% of ovarian malignant lesions). The strong KDR-targeted US signal was present in 77% and 93% of ovarian and breast malignant lesions respectively. Although not designed to measure accuracy, the results were encouraging for further continued testing. Smeenge and co-workers recently conducted a phase 0 study in prostate cancer (PCa) patients to assess the feasibility and safety of BR55 in detecting PCa lesions [9]. Upon improving scanning settings, 68% of PCa lesions detected by histology after prostatectomy were localized through BR55 US imaging ($n = 12$). These pilot results show promise in the utility of US molecular imaging in differentiating between malignant and benign lesions making it an important tool to help reduce unnecessary biopsies or surgeries in the future.

Nano-sized UCAs (nUCAs)

One major limitation in targeted molecular US imaging is the lack of submicron-size UCAs which can still amplify the US contrast as well as extravasate beyond the vasculature to target disease biomarkers (e.g. on tumor cells) directly (Figure 1b). Unfortunately, reducing the size of the MBs not only reduces its echogenicity under clinical ultrasound but also reduces the stability of gas-filled bubbles in solution [10]. This makes it extremely challenging to develop small yet highly echogenic particles resulting in the need to exploit other non-traditional strategies to develop nUCAs. A variety of nUCAs have been developed/discovered which enabled new, paradigm shifting applications of CEUS in diagnosis and therapy (theranostics) [11–14]. Such agents include chemical-based agents (developed from organic and/or inorganic material) as well as genetically engineered protein-shelled particles (such as gas vesicles) [15,16••]. A wide range of echogenic nUCAs with an inorganic shell have been reported and are reviewed elsewhere [12,17••,

18●]. The following sections will highlight novel efforts (2015-present) in developing organic nUCAs. While many of these agents are employed for both imaging and therapeutic applications, the focus of this review will be more towards their utility and potential as molecular ultrasound imaging agents.

Organic nUCAs

The advancements in nanomedicine resulted in a rapid development of echogenic and biocompatible organic nUCAs (50–600 nm) with promising physical properties. These particles are composed of a phospholipid-based shell and/or polymer-based shell and a solid, liquid or gas core (Figure 2). Prominent examples in this direction are summarized in Table 1 with a few reports highlighted in the following sections of the article.

Gas-filled nanobubbles (NBs)

NBs are nanoparticles (diameter < 1 μm) comprised from a phospholipid shell stabilized by a surfactant and a perfluorocarbon gas core (Figure 2a). A number of publications reported the development of NBs actively targeted to extracellular markers of cancer [19,20,21●]. Yang *et al.* and Fan *et al.* developed NBs targeted to human epidermal growth factor receptor type 2 (HER2) and prostate specific membrane antigen (PSMA) respectively and took advantage of biotin-streptavidin or avidin interaction to attach the respective targeting moiety to the NBs surface [19,20]. Both groups showed effective targeting of the NBs by measuring the increase in US signal. Unfortunately, these NBs showed limited *in vivo* stability (2 and 20 min respectively) and are not clinically translatable due to the use of immunogenic avidin/streptavidin. Jiang *et al.* later developed more clinically translatable HER2-targeted NBs by covalently attaching the targeting moiety (Herceptin) to the surface of the NBs [21●]. These NBs are slightly bigger in diameter (613.0 ± 25.4 nm) but showed target-specific US signal enhancement in HER2-expressing tumors for up to 40 min. Although NB's extravasation was confirmed through histology, the pore gaps in tumors are usually very heterogeneous and validating extravasation on other tumor models is necessary [22]. Recently, Gao and coworkers prepared NBs targeted to ovarian cancer by covalently coupling CA-125 antibody to the surface of the NBs [23]. *In vivo* evaluation showed over two-fold higher US signal in CA-125 positive tumor xenograft (OVCAR-3) compared to non-targeted NBs but US monitoring was only conducted for 10 min.

Efforts by Perera and co-workers looked into adding a crosslinking polymer to the phospholipid-based NBs to reduce the diffusion of the perfluorocarbon gas core thus stabilizing the NBs without affecting the flexibility of its shell (i.e. reduce US contrast ability) [24]. After UV irradiation to activate the cross coupling reaction, the NBs showed better *in vivo* stability and passive tumor targeting than NBs without the cross-linker but only seven minutes of *in vivo* monitoring was conducted.

Phase-change droplets (PCDs)

Nanodroplets (NDs) are comprised of a low boiling liquid perfluorocarbon encapsulated within an organic or inorganic shell (Figure 2b) [11,12]. The advantage of such nano-

emulsions is their ability to preserve their shape and initial diameter upon injection and undergo a liquid-to-gas transition once exposed to high energy (heat) producing micron-sized bubbles at the site(s) of interest. This allows NDs to extravasate and accumulate at the site of disease before transforming into echogenic bubbles upon heating [11,12]. The activation can occur upon exposure to US-, NIR-, magnetic-irradiation, radio-irradiation and microwave-irradiation and the majority of novel NDs are developed through thin film hydration (phospholipid–based) or water/oil/water formulation (W/O/W; polymer-based) [25,26]. In addition, several reports looked into developing NDs from premade micron-sized particles through condensation by increasing ambient pressure and/or decreasing the temperature [27]. Such an approach can be very useful to prepare NDs from existing commercial CAs which can avoid the need for in-house synthesis, minimize resource requirements and possibly improve particle yield.

Acoustic droplet vaporization (ADV)

As the name implies, these nanoparticles are transformed into MBs upon heating caused by exposure to ultrasound. Li and co-workers developed perfluorooctyl bromide (PFOB) nanodroplets coated with a folic acid-conjugated chitosan/alginate-PEG layer [28••]. *In vivo* evaluation of the targeted NDs showed higher US signal enhancement in the folate receptor-expressing tumors compared to non-expressing tumors or non-targeted NDs. The NDs showed the highest signal enhancement at 20 min postinjection and the signal was detectable for up to 160 min. Similarly, Liu and co-workers developed perfluoropentane (PFP) droplets stabilized by a phospholipid shell [25]. These NDs were also targeted to folate receptor and showed higher US contrast compared to controls when imaged 1 hour post injection. Recently, Choi and co-workers developed a functionalized chitosan-based PFP NDs for multimodal X-ray/CT and US imaging [29••]. The NDs accumulated passively in the tumor and showed peak US signal enhancement at 12 hours with a detectable signal for up to 24 hours.

Other efforts focused on further stabilizing NDs to ensure no premature activation occurs *in vivo* before reaching the disease site. Huang and co-workers developed polymerbased ADV NPs which are further stabilized with a UVinduced thiolene crosslinking moiety [30]. *In vitro* stability and US characterization showed better stability and less pre-mature vaporization of these particles at room temperature. Picheth and co-workers synthesized a variety of PLA polymers with different fluoro-carbonyl groups to study its effect on stabilizing perfluorocarbon NDs [31]. *In vitro* evaluation showed that the echogenicity of NDs with a fluorinated-shell was increased by at least 3-fold and up to 40-fold compared to ones without the fluorinated shell.

Optical droplet vaporization (ODV)

ODV relies on the availability of a photo-absorber within the NDs which produces heat upon NIR irradiation. A variety of NDs have been reported which incorporate fluorescent dyes or NPs as photo-absorbers. To our knowledge, no CEUS imaging of actively targeted NDs using ODV has been reported and the majority of these particles were evaluated after passive accumulation in the tumor or after intra-tumoral injection in the tumor bed. Zhao *et al.* and

Xu *et al.* reported the development of PLGA-based NPs infused with perfluorohexane (PFH) or PFP NDs respectively [26,32]. The photo-absorber in both cases were iron oxide NPs encapsulated within the NDs which provided means for MRI and CEUS imaging. *In vivo* evaluation of these droplets upon intra-tumoral injection showed CEUS after NIR irradiation. A couple of NDs were also developed for the detection and therapy of tumor sentinel lymph nodes (SNL) [33,34]. For example, Yang and co-workers developed PLGA-based NPs encapsulated with PFH and carbon nanoparticles which produce heat upon NIR irradiation [34]. *In vivo* evaluation in rabbits bearing a VX2 tumor showed the accumulation of these NDs in popliteal fossa lymph nodes using both photoacoustic and CEUS imaging with a detectable US signal for up to two hours. Finally, two reports relied on producing fluorescent NDs (porphyrin or Cy7.5 respectively) from micron-sized bubbles through pressurization [35,36]. Paproski and co-workers showed passive accumulation (EPR) of their porphyrin NDs in a HT1080 tumor model in chicken embryo [35]. On the other hand, Lin and co-workers assessed their NDs *in vitro* showing around 11 times higher US signal enhancement upon NIR irradiation compared to dye-less NDs [36].

Due to the easy scattering of US by gas or bone as well as the limited penetration-depth of NIR, investigators looked into exploring other means to activate NDs. A number of publications investigated utilizing magnetic, radio or microwave irradiation to activate NDs and conducted preliminary evaluations upon intra-tumoral injection in mice. Zhou and co-workers developed hollow iron oxide nanoparticles (HIONs) which are encapsulated with PFH through a vacuum-assisted impregnation process [37]. Such particles were able to produce heat upon magnetic stimulation and showed 1.7-fold increase in US signal after magnetic irradiation for 3 min. Zhang and coworkers developed PLGA-based NPs infused with DL-menthol which was activated upon radiofrequency irradiation [38]. Lastly, Xu and co-workers developed folatetargeted phospholipid-based particles infused with a mixture of PFH and PFP [39]. Activation of such NDs was conducted upon microwave irradiation and bubble production was visible using CEUS imaging.

Gas-generating NPs (GGNPs)

GGNPs consist of nanoparticles incorporating a reactive moiety which produces gas (e.g. CO_2 or O_2) upon reaching site of disease. Figure 2c is a summary of the different functional groups and their gas-production mechanisms which either rely on unique features in the tumor microenvironment (such as low pH or high concentrations of hydrogen peroxide) or require heating. A couple of GGNPs possessing the gas producing functional group on the shell have been reported (Figure $2C_a$). Min and co-workers developed PLGA-based GGNPs functionalized with a carbonate copolymer which produces CO_2 gas upon hydrolysis [40●●] (Figure $2C_{a1}$). After intravenous injection in tumor bearing mice, the NPs passively accumulated in the tumor and CO_2 gas production was monitored using CEUS for up to 4 hours. Kang and co-workers developed GGNPs from poly (vanillin oxalate) which is shown to react with hydrogen peroxide producing CO_2 gas [41●●] (Figure $2C_{a2}$). These particles were evaluated in an animal model with an induced hepatic IR injury and showed enormous potential as an imaging agent for oxidative stress with real time US imaging for up to 1 hour.

Several reports also highlight the use of NPs encapsulated with a base (e.g. ammonium bicarbonate or calcium carbonate) which produce CO_2 gas in acidic environments (Figure $2_{b1–3}$) [42–48]. Zhang and co-workers incorporated ammonium bicarbonate and gold nanorods (GNRs) in phospholipid-based NPs and showed the ability to produce CO2 gas at the tumor site upon heating caused by NIR-irradiation [42]. The large amounts of CO_2 gas was detectable *in vivo* via CEUS for up to 4 hours. Kim *et al.* developed an alginate loaded nanocarrier which was used as a vessel where $CaCO_3$ was produced [44]. These nanoparticles passively accumulated in the tumor after intravenous injection and showed US signal enhancement for up to 60 min. Lee and co-workers developed PLGA-particles loaded with $CaCO_3$ targeted to neuroblastoma using a rabies virus glycoprotein peptide [46]. Such particles were able to specifically target neuroblastoma tumors and showed US signal enhancement for up to 30 min.

Lastly, GGNPs can also produce O_2 gas from hydrogen peroxide either through enzymatic activation or by reacting with MnO_2 (Figure $2C_{b4–5}$). Wang and co-workers developed a probe composed of functionalized superparamagnetic iron oxide particles, a dual enzyme species (catalase and superoxide dismutase), and a polysaccharide cationic polymer glycol chitosan gel [49]. These agents were passively targeted to VX2 tumors in rabbits upon intravenous injection via the ear vein and O2 production was monitored for up to 2 hours using ultrasound. In addition, Gao and co-workers recently developed a theranostic agent from HA-NPs encapsulated with ICG and MnO_2 to help provide more oxygen at the tumor site during photodynamic therapy (PDT) [50●●]. *In vivo* results in tumor bearing mice showed enhanced US signal in the tumor for up to 24 hours post intravenous injection.

Conclusion

With the development and preliminary clinical assessment of targeted US contrast agents, US imaging is showing great potential as a molecular US imaging modality. This concise review highlights some creative approaches in developing novel nUCAs. Whether for imaging or therapy, the development and complete evaluation of nUCAs requires a lot of chemistry expertise, knowledge about biological systems and a foundational background in US physics. This further enforces the need for cross discipline collaborations in order to develop and properly evaluate nUCAs as US molecular imaging agents. While many of the highlighted nUCAs show immense promise, these agents are fairly recent and more studies are required to better assess their clinical utility and safety profile. Furthermore, the ability of NBs to enhance US contrast at clinically relevant frequencies is not well understood and further US physical assessments are needed. Similarly, studies that can correlate the US signal enhancement with biomarker expression using nUCAs (especially when using PCDs or GGNPs) are important to showcase their potential as molecular imaging agents. While still in its early phase, developments of stable nUCAs with the appropriate instrumentation and US sequences are slowly evolving and will serve as a focal point for the fast growth of molecular US imaging.

Acknowledgements

This work was supported in part by NCI ICMIC P50CA114747 (SSG), NCI RO1 CA082214 (SSG), NCI RO1 CA135486 (SSG), NCI CCNE-TR U54 CA119367 (SSG), CCNE-T U54 U54CA151459, NIBIB BRP 5-RO1-

EBB000312 (SSG), NCI U01 EDRN CA152737, DOE DE-SC0008397 (SSG), NCI 1 R21 CA178360, Canary Foundation, Ben & Catherine Ivy Foundation, and Sir Peter Michael Foundation.

References and recommended reading

Papers of particular interest, published within the period of review, have been highlighted as:

● of special interest

●● of outstanding interest

1. James ML, Gambhir SS: A molecular imaging primer: modalities, imaging agents, and applications. Physiol Rev 2012, 92:897–965. [PubMed: 22535898]
2. Cosgrove D, Harvey C: Clinical uses of microbubbles in diagnosis and treatment. Med Biol Eng Comput 2009, 47:813–826. [PubMed: 19205774]
3. Ignee A, Atkinson NSS, Schuessler G, Dietrich CF: Ultrasound contrast agents. Endosc Ultrasound 2016, 5:355–362. [PubMed: 27824024]
4. Wilson SR, Burns PN: Microbubble-enhanced US in body imaging: what role? Radiology 2010, 257:24–39. [PubMed: 20851938]
5●. Abou-Elkacem L, Bachawal SV, Willmann JK: Ultrasound molecular imaging: moving toward clinical translation. Eur J Radiol 2015, 84:1685–1693. [PubMed: 25851932] A great review summarizing the application of molecular ultrasound imaging.
6. Kiessling F, Fokong S, Bzyl J, Lederle W, Palmowski M, Lammers T: Recent advances in molecular, multimodal and theranostic ultrasound imaging. Adv Drug Deliv Rev 2014, 72:15–27. [PubMed: 24316070]
7. Pochon S, Tardy I, Bussat P, Bettinger T, Brochot J, Wronski von M, Passantino L, Schneider M: BR55: a lipopeptide-based VEGFR2-targeted ultrasound contrast agent for molecular imaging of angiogenesis. Invest Radiol 2010, 45:89–95. [PubMed: 20027118]
8●●. Willmann JK, Bonomo L, Carla Testa A, Rinaldi P, Rindi G, Valluru KS, Petrone G, Martini M, Lutz AM, Gambhir SS: Ultrasound molecular imaging with BR55 in patients with breast and ovarian lesions: first-in-human results. J Clin Oncol 2017 10.1200/JCO.2016.70.8594.The First in human evaluation of molecular ultrasound imaging.
9. Smeenge M, Tranquart F, Mannaerts CK, de Reijke TM, van de Vijver MJ, Laguna MP, Pochon S, la Rosette de JJMCH, Wijkstra H: First-in-human ultrasound molecular imaging with a VEGFR2-specific ultrasound molecular contrast agent (BR55) in prostate cancer: a safety and feasibility pilot study. Invest Radiol 2017, 52:419–427. [PubMed: 28257340]
10. Sheeran PS, Streeter JE, Mullin LB, Matsunaga TO, Dayton PA: Toward ultrasound molecular imaging with phase-change contrast agents: an in vitro proof of principle. Ultrasound Med Biol 2013, 39:893–902. [PubMed: 23453380]
11. Güvener N, Appold L, de Lorenzi F, Golombek SK, Rizzo LY, Lammers T, Kiessling F: Recent advances in ultrasound-based diagnosis and therapy with micro-and nanometer-sized formulations. Methods 2017, 130:4–13. [PubMed: 28552267]
12. Tang H, Zheng Y, Chen Y: Materials chemistry of nanoultrasonic biomedicine. Adv Mater 2017, 29:1604105.
13. Huynh E, Rajora MA, Zheng G: Multimodal micro, nano, and size conversion ultrasound agents for imaging and therapy. WIREs Nanomed Nanobiotechnol 2016, 8:796–813.
14. Perera RH, Hernandez C, Zhou H, Kota P, Burke A, Exner AA: Ultrasound imaging beyond the vasculature with new generation contrast agents. WIREs Nanomed Nanobiotechnol 2015, 7:593–608.
15. Shapiro MG, Goodwill PW, Neogy A, Yin M, Foster FS, Schaffer DV, Conolly SM: Biogenic gas nanostructures as ultrasonic molecular reporters. Nat Nanotechnol 2014, 9:311–316. [PubMed: 24633522]
16●●. Bourdeau RW, Lee-Gosselin A, Lakshmanan A, Farhadi A, Kumar SR, Nety SP, Shapiro MG: Acoustic reporter genes for noninvasive imaging of microorganisms in mammalian hosts. Nature

2018, 553:86–90. [PubMed: 29300010] Utility of genetically engineered protein gas vesicles for in vivo US imaging of microorganisms.

17●●. Qian X, Han X, Chen Y: Insights into the unique functionality of inorganic micro/nanoparticles for versatile ultrasound theranostics. Biomaterials 2017, 142:13–30. [PubMed: 28719818] A great review summarizing different types of inorganic UCAs.

18●. Zhou Y, Han X, Jing X, Chen Y: Construction of silica-based micro/nanoplatforms for ultrasound theranostic biomedicine. Adv Healthc Mater 2017, 6:1700646.A great review highlighting silica-based UCA's development and utility as ultrasound theranostic agents.

19. Yang H, Cai W, Xu L, Lv X, Qiao Y, Li P, Wu H, Yang Y, Zhang L, Duan Y: Nanobubble–affibody: novel ultrasound contrast agents for targeted molecular ultrasound imaging of tumor. Biomaterials 2015, 37:279–288. [PubMed: 25453958]

20. Fan X, Wang L, Guo Y, Tu Z, Li L, Tong H, Xu Y, Li R, Fang K: Ultrasonic nanobubbles carrying anti-PSMA nanobody: construction and application in prostate cancer-targeted imaging. PLOS ONE 2015, 10:e0127419. [PubMed: 26111008]

21●. Jiang Q, Hao S, Xiao X, Yao J, Ou B, Zhao Z, Liu F, Pan X, Luo B, Zhi H: Production and characterization of a novel long-acting Herceptin-targeted nanobubble contrast agent specific for Her-2-positive breast cancers. Breast Cancer 2015, 23:445–455. [PubMed: 25691133] Development of HER2-targeted NBs with US in vivo detection for up to 40 min.

22. Yuan F, Dellian M, Fukumura D, Leunig M, Berk DA, Torchilin VP, Jain RK: Vascular permeability in a human tumor xenograft: molecular size dependence and cutoff size. Clin Cancer Res 1995, 55:3752–3756.

23. Gao Y, Hernandez C, Yuan H-X, Lilly J, Kota P, Zhou H, Wu H, Exner AA: Ultrasound molecular imaging of ovarian cancer with CA-125 targeted nanobubble contrast agents. Nanomed: Nanotechnol Biol Med 2017, 13:2159–2168.

24. Perera RH, Wu H, Peiris P, Hernandez C, Burke A, Zhang H, Exner AA: Improving performance of nanoscale ultrasound contrast agents using N,N-diethylacrylamide stabilization. Nanomed: Nanotechnol Biol Med 2017, 13:59–67.

25. Liu J, Shang T, Wang F, Cao Y, Hao L, Ren J, Ran H, Wang Z, Li P, Du Z: Low-intensity focused ultrasound (LIFU)-induced acoustic droplet vaporization in phase-transition perfluoropentane nanodroplets modified by folate for ultrasound molecular imaging. Int J Nanomed 2017, 12:911–923.

26. Zhao Y, Song W, Wang D, Ran H, Wang R, Yao Y, Wang Z, Zheng Y, Li P: Phase-shifted PFH@PLGA/Fe3O4 Nanocapsules for MRI/US imaging and photothermal therapy with near-infrared irradiation. ACS Appl Mater Interfaces 2015, 7:14231–14242. [PubMed: 26067333]

27. Sheeran PS, Yoo K, Williams R, Yin M, Foster FS, Burns PN: More than bubbles: creating phase-shift droplets from commercially available ultrasound contrast agents. Ultrasound Med Biol 2017, 43:531–540. [PubMed: 27727022]

28●●. Li K, Liu Y, Zhang S, Xu Y, Jiang J, Yin F, Hu Y, Han B, Ge S, Zhang L et al.: Folate receptor-targeted ultrasonic PFOB nanoparticles: synthesis, characterization and application in tumor-targeted imaging. Int J Mol Med 2017, 39:1505–1515. [PubMed: 28487935] Development of Folate receptor-targeted phase-change droplets with in vivo US detection time for up to 160 min.

29●●. Choi D, Jeon S, You DG, Um W, Kim JY, changes HY: 2008: iodinated echogenic glycol chitosan nanoparticles for X-ray CT/US dual imaging of tumor. Nanotheranostics 2018, 2:117–127. [PubMed: 29577016] Latest report of a multimodal phase-change droplet with up to 24 hours of ultrasound in vivo monitoring.

30. Huang Y, Vezeridis AM, Wang J, Wang Z, Thompson M, Mattrey RF, Gianneschi NC: Polymer-stabilized perfluorobutane nanodroplets for ultrasound imaging agents. J Am Chem Soc 2017, 139:15–18. [PubMed: 28032757]

31. Picheth G, Houvenagel S, Dejean C, Couture O, Alves de Freitas R, Moine L, Tsapis N: Echogenicity enhancement by end-fluorinated polylactide perfluorohexane nanocapsules: towards ultrasound-activable nanosystems. Acta Biomater 2017, 64:313–322. [PubMed: 28986300]

32. Xu Y, Niu C, An S, Tang S, Xiao P, Peng Q, Wang L: Thermal-sensitive magnetic nanoparticles for dual-modal tumor imaging and therapy. RSC Adv 2017, 7:40791–40802.

33. Hannah AS, Luke GP, Emelianov SY: Blinking phase-change nanocapsules enable background-free ultrasound imaging. Theranostics 2016, 6:1866–1876. [PubMed: 27570556]

34. Yang L, Cheng J, Chen Y, Yu S, Liu F, Sun Y, Chen Y, Ran H: Phase-transition nanodroplets for real-time photoacoustic/ ultrasound dual-modality imaging and photothermal therapy of sentinel lymph node in breast cancer. Sci Rep 2017, 7:45213. [PubMed: 28338071]

35. Paproski RJ, Forbrich A, Huynh E, Chen J, Lewis JD, Zheng G, Zemp RJ: Porphyrin nanodroplets: sub-micrometer ultrasound and photoacoustic contrast imaging agents. Small 2016, 12:371–380. [PubMed: 26633744]

36. Lin S, Shah A, Hernández-Gil J, Stanziola A, Harriss BI, Matsunaga TO, Long N, Bamber J, Tang M-X: Optically and acoustically triggerable sub-micron phase-change contrast agents for enhanced photoacoustic and ultrasound imaging. Photoacoustics 2017, 6:26–36. [PubMed: 28507898]

37. Zhou Y, Wang R, Teng Z, Wang Z, Hu B, Kolios M, Chen H, Zhang N, Wang Y, Li P et al.: Magnetic nanoparticle-promoted droplet vaporization for in vivo stimuli-responsive cancer theranostics. NPG Asia Mater 2016, 8:e313.

38. Zhang K, Li P, Chen H, Bo X, Li X, Xu H: Continuous cavitation designed for enhancing radiofrequency ablation via a special radiofrequency solidoid vaporization process. ACS Nano 2016, 10:2549–2558. [PubMed: 26800221]

39. Xu J, Chen Y, Deng L, Liu J, Cao Y, Li P, Ran H, Zheng Y, Wang Z: Microwave-activated nanodroplet vaporization for highly efficient tumor ablation with real-time monitoring performance. Biomaterials 2016, 106:264–275. [PubMed: 27573134]

40●●. Min HS, Son S, You DG, Lee TW, Lee J, Lee S, Yhee JY, Lee J, Han MH, Park JH et al.: Chemical gas-generating nanoparticles for tumor-targeted ultrasound imaging and ultrasound-triggered drug delivery. Biomaterials 2016, 108:57–70. [PubMed: 27619240] Development of a theranostic GGNPs with ultrasound-detectable gas production for up to 4 hours.

41●●. Kang C, Cho W, Park M, Kim J, Park S, Shin D, Song C, Lee D: H2O2-triggered bubble generating antioxidant polymeric nanoparticles as ischemia/reperfusion targeted nanotheranostics. Biomaterials 2016, 85:195–203. [PubMed: 26874282] A great example of a theranostic nanoparticle for ultrasound imaging and treatment of IR injury.

42. Zhang N, Li J, Hou R, Zhang J, Wang P, Liu X, Zhang Z: Bubble-generating nano-lipid carriers for ultrasound/CT imaging-guided efficient tumor therapy. Int J Pharm 2017, 534:251–262. [PubMed: 28803939]

43. Feng G, Hao L, Xu C, Ran H, Zheng Y, Li P, Cao Y, Wang Q, Xia J, Wang Z: High-intensity focused ultrasound-triggered nanoscale bubble-generating liposomes for efficient and safe tumor ablation under photoacoustic imaging monitoring. Int J Nanomed 2017, 12:4647–4659.

44. Kim M, Lee JH, Kim SE, Kang SS, Tae G: Nanosized ultrasound enhanced-contrast agent for in vivo tumor imaging via intravenous injection. ACS Nano 2016, 8:8409–8418.

45. Feng Q, Zhang W, Yang X, Li Y, Hao Y, Zhang H, Hou L, Zhang Z: pH/ultrasound dual-responsive gas generator for ultrasound imaging-guided therapeutic inertial cavitation and sonodynamic therapy. Adv Healthc Mater 2017, 139:1700957.

46. Lee J, Min HS, You DG, Kim K, Kwon IC, Rhim T, Lee KY: Theranostic gas-generating nanoparticles for targeted ultrasound imaging and treatment of neuroblastoma. J Control Release 2016, 223:197–206. [PubMed: 26739549]

47. Park DJ, Min KH, Lee HJ, Kim K, Kwon IC, Jeong SY, Lee SC: Photosensitizer-loaded bubble-generating mineralized nanoparticles for ultrasound imaging and photodynamic therapy. J Mater Chem B 2016, 4:1219–1227.

48. Gaspar VM, Moreira AF, Costa EC, Queiroz JA, Sousa F, Pichon C, Correia IJ: Gas-generating TPGS-PLGA microspheres loaded with nanoparticles (NIMPS) for co-delivery of minicircle DNA and anti-tumoral drugs. Colloids Surf B Biointerfaces 2015, 134:287–294. [PubMed: 26209779]

49. Wang X, Niu D, Li P, Wu Q, Bo X, Liu B, Bao S, Su T, Xu H, Wang Q: Dual-enzyme-loaded multifunctional hybrid nanogel system for pathological responsive ultrasound imaging and T2-weighted magnetic resonance imaging. ACS Nano 2015, 9:5646–5656. [PubMed: 26035730]

50●●. Gao S, Wang G, Qin Z, Wang X, Zhao G, Ma Q, Zhu L: Oxygen-generating hybrid nanoparticles to enhance fluorescent/ photoacoustic/ultrasound imaging guided tumor photodynamic therapy. Biomaterials 2017, 112:324–335. [PubMed: 27776285] Development of

oxygen-generating nanoparticles for multimodal ima-ging, enhancing efficacy of photodynamic therapy and up to 24 hours of US in vivo monitoring.

51. Min HS, You DG, Son S, Jeon S, Park JH, Lee S, Kwon IC, Kim K: Echogenic glycol chitosan nanoparticles for ultrasound-triggered cancer theranostics. Theranostics 2015, 5:1402–1418. [PubMed: 26681985]
52. Cheng Y, Cheng H, Jiang C, Qiu X, Wang K, Huan W, Yuan A, Wu J, Hu Y: Perfluorocarbon nanoparticles enhance reactive oxygen levels and tumour growth inhibition in photodynamic therapy. Nat Commun 2015, 6:8785. [PubMed: 26525216]
53. Min KH, Min HS, Lee HJ, Park DJ, Yhee JY, Kim K, Kwon IC, Jeong SY, Silvestre OF, Chen X et al.: pH-controlled gas-generating mineralized nanoparticles: a theranostic agent for ultrasound imaging and therapy of cancers. ACS Nano 2015, 9:134–145. [PubMed: 25559896]

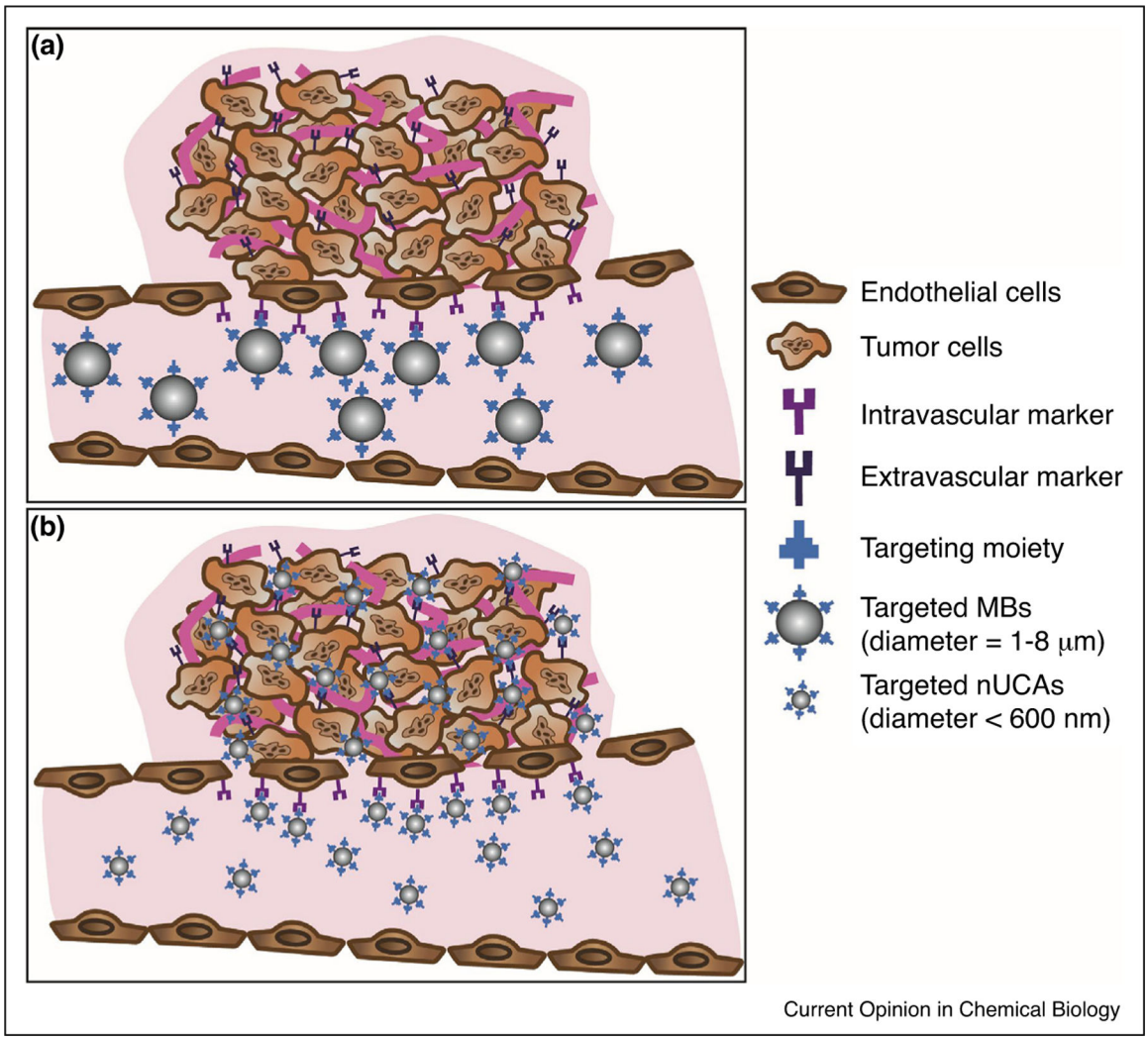

Figure 1.

Schematic representation of molecular US imaging using micro-sized and nano-sized UCAs (MBs and nUCAs respectively). **(a)** Molecular US imaging using targeted MBs which are limited to the vascular space and can only target intravascular markers of cancer due to inability to extravasate into tumor microenvironment. **(b)** Molecular US imaging using targeted nUCAs which can actively target intravascular and extravascular markers of cancer as well as passively accumulate in the tumor microenvironment through the enhanced pore and retention effect (EPR).

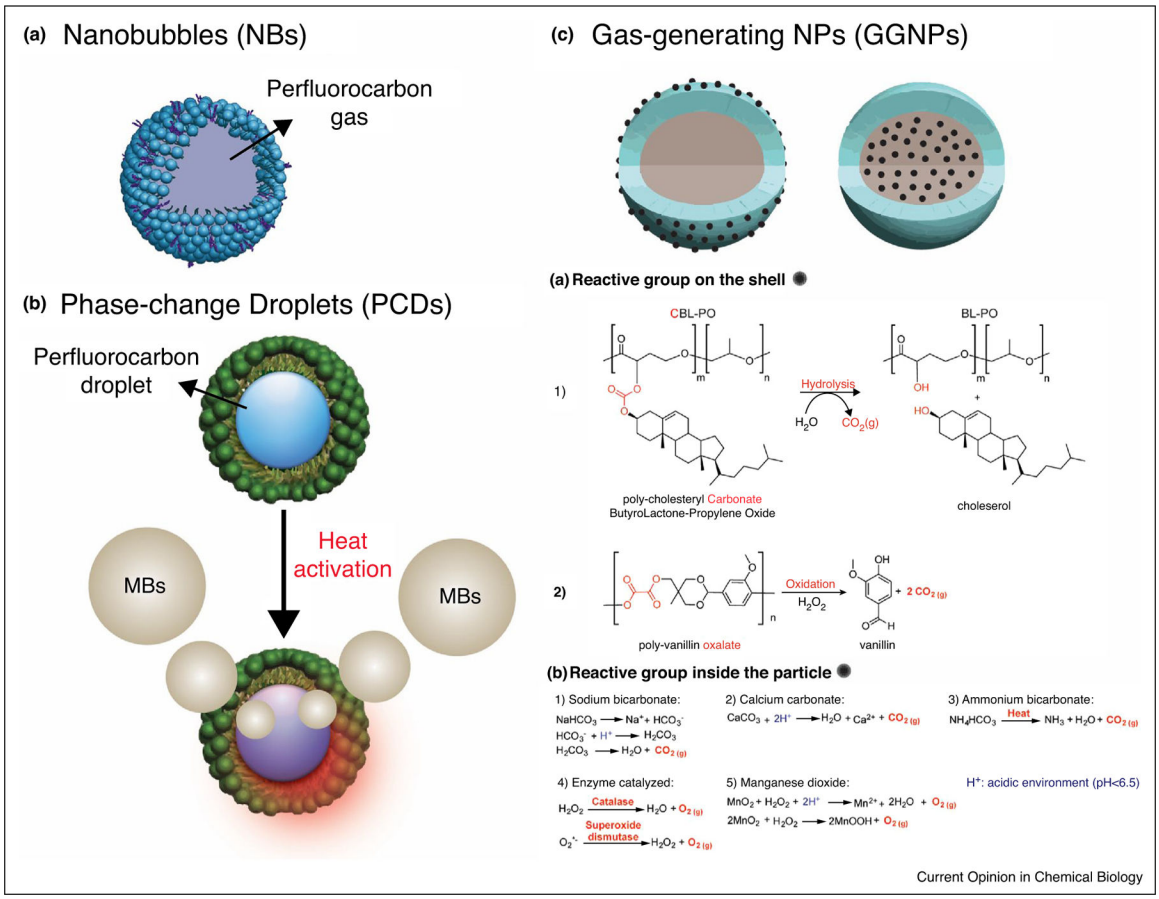

Figure 2.

Schematic representation summarizing novel organic nUCAs. **(a)** Nanobubbles (NBs): perfluorocarbon gas-filled particles stabilized with a phospholipid shell (blue) and surfactant (purple). **(b)** Phase-change droplets (PCDs): perfluorocarbon droplets encapsulated in phospholipid or polymer-based (green) NPs. Phase-change of droplets occurs upon heating caused by ultrasound, near infrared, magnetic, radio-wave or microwave irradiation. **(c)** Gas-generating NPs (GGNPs): NPs containing a reactive functional group which produces gas at the site of interest. Reactive group can either be placed on the shell (Left) or inside the NPs (Right). C_a and C_b summarize the different mechanisms used to produce gas in GGNPs.

Table 1

Summary of reported organic nUCAs (2015–2018)

Diameter (nm)		Composition	Core	Ref.	Target strategy	Monitoring time
Nanobubbles (NBs)						
	478 ± 29	biotin-PEG-DSPE, DPPC, glycerol	OFP (g)	[19]	HER2 (affibody)	~2 min
	487 ± 33	biotin-PEG-DSPE, DPPC, DPPA, glycerol	OFP (g)	[20]	PSMA (nanobody)	~23 min
	613 ± 25	DSPE-PEG-COOH, DPPE, DSPC, PEG_{4000}	OFP (g)	[21●]	HER2 (herceptin)	~40 min
	74 ± 16	DPPC, DPPA, DPPE, DSPE-PEG-COOH, pluronic L10, glycerol	OFP (g)	[23]	CA-125 (antibody)	~10 min
	95 ± 25	DPPC, DPPA, DPPE, mPEG-DSPE, pluronic; NNDEA, BAC, Irgacure 2959	OFP (g)	[24]	EPR	~7 min
Phase-change droplets (PCDs)						
ADV	301 ± 10	FA-chitosan, alginate-PEG_{3400}, egg lecithin, cholesterol	PFOB (l)	[28●●]	Folate receptor (folic acid)	~2.6 hours
	321 ± 67	HSPC, DSPE-PEG-Folate, DPPG, cholesterol	PFP (l)	[25]	Folate receptor (folic acid)	NA
	454 ± 3	DTA-glycol chitosan	PFP (l)	[29●●]	EPR	~24 hours
	152 – 158	PLA-C_nF_{2n+1}; n = 3, 6, 8, 11 and 13; sodium cholate	PFH (l)	[31]	NA	NA
	432 ± 32	glycol chitosan, 5β-cholanic acid	PFP (l)	[51]	EPR	~60 min
ODV	~374	PLGA, oleic-acid-coated Fe_3O_4 NPs, PVA	PFH (l)	[26]	Intra-tumor injection	~ 5 min
	~294	PLGA, oleic-acid-coated Fe_3O_4 NPs, PVA	PFP (l)	[32]	Intra-tumor injection	~ 4 min
	~200	zonyl FSO fluorosurfactant; Epolight 3072	PFH (l)	[33]	Sentinel lymph node	NA
	435 ± 41	PLGA, Carbon NPs, PVA	PFH (l)	[34]	Sentinel lymph node	~ 2 hrs
	185 ± 39	SPPG-PC, DSPC, DSPE-PEG-amine; porphyrin	PFB (l)	[35]	EPR	NA
	~400	DPPC, DSPE-PEG, DSPE-PEG-Cy7.5, propylene glycol, glycerol	DFB (l)	[36]	NA	NA
	~200	DSPE-PEG, lecithin, cholesterol; IR780	PFH (l)	[52]	EPR	NA
MDV	~600	HIONs	PFH (l)	[37]	Intra-tumor injection	NA
RfDV	~450	PLGA, PVA	DL-menthol	[38]	Intra-tumor injection	NA
MWDV	132 ± 78	DPPC, DSPE-PEG-Folate, DPPG, cholesterol	PFP + PFH (l)	[39]	Intra-tumor injection (Folate Receptor)	~10 min
Gas-generating nanoparticles (GGNPs)						
CO_2 (g)	290 ± 18	Poly($[CBL]_{75}$-$[PO]_{25}$)/PLGA, Pluronic F68		[40●●]	EPR	~4 hours
	~550	PVO, PVA		[41●●]	Hepatic IR injury	~60 min
	152 ± 0.6	DSPE-PEG-FA, lecithin, cholesterol; GNR	NH_4HCO_3	[42]	Folate Receptor (folic acid)	~4 hours
	174 ± 58	DPPC, DSPE-PEG, cholesterol	NH_4HCO_3	[43]	EPR	NA

	Diameter (nm)	Composition	Core	Ref.	Target strategy	Monitoring time
	~160	Diacrylated-pluronic F127, alginate	$CaCO_3$	[44]	EPR	~60 min
	~250	Mesoporous $CaCO_3$ NPs, HMME, HA	$CaCO_3$	[45]	EPR	NA
	~220	PLGA, PVA	$CaCO_3$	[46]	Neuroblastoma (RVGP)	~30 min
	354 ± 59	pAsp-PEG; Ce6	$CaCO_3$	[47]	NA	NA
	180 ± 15	PLGA, L-histidine and L-arginine modified chitosan, PVA	mcDNA; $NaHCO_3$	[48]	NA	NA
	240 ± 8	pAsp-PEG	$CaCO_3$	[53]	Intra-tumor injection	~2 hours
O_2 (g)	~218	SPIO, polymer glycol chitosan gel	CAT; SOD	[49]	EPR	~2 hours
	239 ± 4	HA, 5β-cholanic acid	MnO_2 and ICG	[50●●]	EPR	~24 hours

Abbreviations: ADV: acoustic droplet vaporization; BAC: N,N-bis(acryoyl) cystamine; CAT: catalase; CA-125: cancer antigen 125; CBL-PO: cholesteryl carbonatebutyrolactone-propylene oxide; DFB: decafluorobutane; DPPA: 1,2-dipalmitoyl-sn-glycero-3-phosphate (sodium salt); DPPC: 1,2-dipalmitoyl-sn-glycero-3-phosphocholine; DPPE: 1,2-dipalmitoyl-sn-glycero-3-phosphoethanolamine; DPPG: 1,2-dipalmitoyl-sn-glycero-3-phospho-(1′ - rac-glycerol) (sodium salt); DSPE: 1,2-distearoyl-sn-glycero-3-phosphoethanolamine; DTA: diatrizoic acid; EPR: enhanced permeability and retention effect; FA: folic acid; GNR: gold nanorods; HA: hyaluronic acid; HER2: human epidermal growth factor receptor 2; HIONs: hollow iron oxide nanoparticles; Hepatic IR injury: hepatic ischemia-reperfusion injury; HMME: hematoporphyrin monomethyl ether; HSPC: L-α-phosphatidylcholine, hydrogenated (Soy); ICG: indocyanine green; MDV: magnetic droplet vaporization; MWDV: microwave droplet vaporization; NNDEA: N,N-diethyl acrylamide; ODV: optical droplet vaporization; OFP: octafluoropropane; pAsp-PEG: Poly(L-aspartic acid)-PEG; PEG: polyethylene glycol; PFB: perfluorobromide; PFH: perfluorohexane; PFOB: perfluorooctyl bromide; PFP: perfluoropentane; p.i: post injection; PLA: polylactic acid; PLGA: poly (lactic-co-glycolic acid); PSMA: prostate specific membrane antigen; PVA: polyvinyl alcohol; PVO: polyvanillin oxalate; RGD: Arginyl glycyl aspartic acid; RfDV: radiofrequency droplet vaporization; ROS: reactive oxygen species; RVGP: Rabies virus glycoprotein peptide; SOD: superoxide dismutase; SPIO: superparamagnetic iron oxide nanoparticles; SPPG-PC: 1-stearoyl-2-pyropheophorbide-sn-glycero-3-phosphocholine.